

# Analysis, Control, and State Estimation for the Networked Competitive Multi-Virus SIR Model

Ciyuan Zhang, Sebin Gracy, Tamer Başar, and Philip E. Paré\*

**Abstract**—This paper proposes a novel discrete-time multi-virus susceptible-infected-recovered (SIR) model that captures the spread of competing epidemics over a population network. First, we provide sufficient conditions for the infection level of all the viruses over the networked model to converge to zero in exponential time. Second, we propose an observation model which captures the summation of all the viruses' infection levels in each node, which represents the individuals who are infected by different viruses but share similar symptoms. Third, we present a sufficient condition for the model to be strongly locally observable, assuming that the network has only infected or recovered individuals. Fourth, we propose a Luenberger observer for estimating the states of our system. We prove that the estimation error of our proposed estimator converges to zero asymptotically with the observer gain. Finally, we present a distributed feedback controller which guarantees that each virus dies out at an exponential rate. We then show via simulations that the estimation error of the Luenberger observer converges to zero before the viruses die out.

## I. INTRODUCTION

The history of human civilization has been a narrative of undergoing, battling, and outmatching various pandemics [2]–[4]. The devastation that epidemics leave in their wake is well-known; as examples, the 2009 swine flu pandemic, which was caused by the H1N1 influenza virus resulted in 60.8 million cases worldwide [5], and the more recent SARS-CoV-2 virus infected 642 million individuals globally [6]. Given the detrimental impacts that epidemics have on society, research on the spread of multiple diseases has attracted attention from several research communities. In fact, research activity has grown massively with the investigation of each epidemic. Various infection models have been proposed and studied in the literature to capture epidemic processes, based on the characteristics of individual pathogens, some of the most basic ones being the susceptible-infected-susceptible (SIS), susceptible-infected-removed (SIR), and susceptible-infected-removed-susceptible (SIRS) models [7]. The SIR model is a simple yet classic epidemic model for diseases in which hosts recover with permanent or close to permanent immunity

following infection [8]. Diseases belonging to this category include a wide range of airborne diseases: Spanish Flu, SARS [9], MERS [10], Influenza [11], H1N1 [12], Ebola [13], and COVID-19 [14], [15], to cite a few.

To make the situation more complicated (and realistic), it is not unusual for multiple viruses/strains to be simultaneously active in a community. When there are multiple viruses circulating, those could either be cooperative, in which case infection increases the likelihood of simultaneous infection with another virus [16], or competitive, in which case infection with one virus precludes the possibility of simultaneous infection with another virus, [17], [18]. Inspired by the competition of different virus strains in population networks [19]–[21], we investigate in this paper the spread of competitive viruses over a population network. Note that the network model can efficiently capture the spread of epidemics over large populations as compared to single-population compartmental models [22]. An extensive amount of effort has been expended on the study of multi-virus models [18], [23]–[30], all of which focus on the competing SIS networked virus model, whereas a susceptible-infected-water-susceptible (SIWS) multi-virus model with a shared resource was investigated in [30]. The competing networked epidemic models can be applied to many fields other than epidemiology, such as modeling the spread of competitive opinions spread over social networks [26], rival merchandise's sales in a market [24], and competing US Department of Agriculture farm subsidy programs [25].

The single virus SIR epidemic networked model has been studied extensively, e.g., [31]–[35]. The competing SIR epidemic model has been investigated in [36]. The focus in [36], however, was on a competing bi-virus (two viruses) SIR epidemic model; it does not account for the networked case nor does it consider an arbitrary but finite number of viruses. To the best of our knowledge, a networked multi-competitive SIR model that accounts for the presence of an arbitrary but finite number of viruses has not yet been studied in the literature. Thus, in this work, we propose a discrete-time multi-competitive networked SIR model. The multi-virus model captures the presence and spread of multiple viruses/variants over a population, such as different variants of SARS-CoV-2 virus, and could also be utilized to represent different behaviors of strains of viruses that compete with each other [37].

Beyond the modeling and analysis of epidemic models, monitoring of epidemics and estimation of infection levels in the population have been some of the fundamental quests in the research on competing contagions. Given that the SARS-CoV-2 pandemic has provided us with an enormous amount of data, the question of how to accurately infer the infection lev-

An earlier version of part of this work was presented at the IFAC Conference on Networked Systems (Necsys22), Zurich, Switzerland [1].

\*Ciyuan Zhang and Philip E. Paré are with the Elmore Family School of Electrical and Computer Engineering at Purdue University, West Lafayette, IN, 47907, USA. Emails: {zhan3375, philpare}@purdue.edu. Sebin Gracy is with the Electrical and Computer Engineering Department at Rice University, Houston, TX, 77005, USA. Email: sebin.gracy@rice.edu. Tamer Başar is with the Coordinated Science Laboratory at the University of Illinois at Urbana-Champaign, Urbana, IL, 61801, USA. Email: basar1@illinois.edu. Research supported in part by the Rice Academy of Fellows, Rice University, and the National Science Foundation, grants NSF-ECCS #2032258 and NSF-ECCS #2032321.

els with respect to various strains of a virus (Delta, Omicron, etc.) and/or with respect to different viruses (influenza, SARS-CoV-2) have been pursued by the research community [38]–[40]. Note that certain infectious diseases, in particular Delta and Omicron variants of the SARS-CoV-2 virus [41], [42] in spite of being competing, exhibit similar symptoms. Consequently, it is quite likely that an individual suffering from the Omicron variant could be diagnosed as having Delta, and vice-versa. Thus, certain competing SIR epidemics can affect the measurement of the cases corresponding to each epidemic and, therefore, pose difficulties for the estimation of the states of each epidemic. When testing facilities are limited, as was witnessed at the beginning of the SARS-CoV-2 pandemic and at various peaks of different waves [43], it is even more difficult to, assuming an individual is infected, accurately infer which virus is it that said individual is infected with [44], [45]. In this paper, we consider the following research question: assuming that there are multiple competing viruses spreading over a network, given measurements of individuals who exhibit symptoms corresponding to at least one (but possibly more) of the viruses, can we accurately estimate the infection level with respect to each virus? State estimation of non-linear systems having a structure similar to SIR epidemic models has been studied in [46]–[48]. However, scenarios where the observation is an accumulation of the system states with a dimension lower than that of the system states have not been investigated in the literature.

In [49], the authors thoroughly investigated a distributed observer for discrete-time LTI networked systems, where the observation model collects measurements of the system states from a node and its neighbors. The paper focused on the LTI systems which do not capture the nonlinear feature of the epidemic systems; it did not consider the scenario when the dimension of the observation vector is lower than the dimension of the state space. However, the distributed approach for observer design in [49] has inspired us to design a distributed estimator which considers the measurements of the local node and the inferred systems states of the neighboring nodes in the network for estimation. Different from [49], we assume that each node (corresponds to a subpopulation in our case) obtains completely accurate information regarding the values that the states of its neighbors take and that, furthermore, there is no time delay.

Note that the discussion so far has focused on the stability analysis, observability, and design of the observer for the model that we have proposed. Yet another challenging problem that policymakers are confronted with during the course of a pandemic is the design of effective eradication/mitigation strategies. As we will show later in the paper, all the viruses in the competing SIR networked model die out eventually regardless of the system parameters. However, the exponential decay of the viruses is essential for the decision-makers as it guarantees that fewer individuals become infected by the virus over the course of the outbreak compared to non-exponential convergence [31]. To the best of our knowledge, distributed feedback control for competing SIR networked epidemic models has remained an open problem- the present paper aims to address this gap as well.

Earlier versions of some of the results in this paper were presented in [1]. This paper substantially expands upon the conference version by:

- deriving a result guaranteeing that the estimation error converges to zero asymptotically (see Theorem 3);
- proposing a distributed mitigation strategy that eradicates all the viruses at an exponential rate, (see Theorem 4); and
- presenting additional simulations which corroborate the theoretical results of the paper and show how to choose the feasible observer gain such that the estimated system states are well-defined.

#### A. Paper Contributions

Through this paper, we make the following contributions:

- i) We propose a discrete-time competitive multi-virus networked SIR model; see Eq. (2).
- ii) We provide sufficient conditions for the infection level of each virus to converge to zero in exponential time; see Theorem 1 and Proposition 1.
- iii) We specify a necessary and sufficient condition that guarantees that the system is strongly locally observable at a certain system state; see Theorem 2.
- iv) We also propose a distributed state estimator and study how to design the observer gain such that the system state estimation errors converge to zero asymptotically; see Theorem 3.
- v) We propose a distributed mitigation algorithm that ensures that the infection level of each virus converges to zero within at least exponential time; see Theorem 4.

#### B. Paper Outline

The paper is organized as follows: Section II proposes a novel discrete-time competitive multi-virus networked SIR model, introduces the research questions addressed in the paper, and provides preliminary results. Section III provides two sufficient conditions for eradication of a virus in exponential time. Section IV examines the observation model, specifies a sufficient condition for the system to be strongly locally observable at a system state (namely, where every node is either in the infected or in the recovered compartment), proposes a distributed Luenberger estimator which estimates the states of the aforementioned model, and determines a condition which ensures that the estimation error of the proposed observer converges to zero asymptotically. Section V proposes a distributed feedback controller that guarantees that each virus dies out at an exponential rate. In Section VI, we utilize simulations to illustrate the results from Sections III, IV, and V. Finally, Section VII summarizes the main findings of the paper.

#### C. Notation

We denote the set of real numbers and the set of non-negative integers by  $\mathbb{R}$  and  $\mathbb{Z}_{\geq 0}$ , respectively. For any positive integer  $n$ , we have  $[n] := \{1, 2, \dots, n\}$ . The spectral radius and an eigenvalue of a matrix  $A \in \mathbb{R}^{n \times n}$  are denoted by

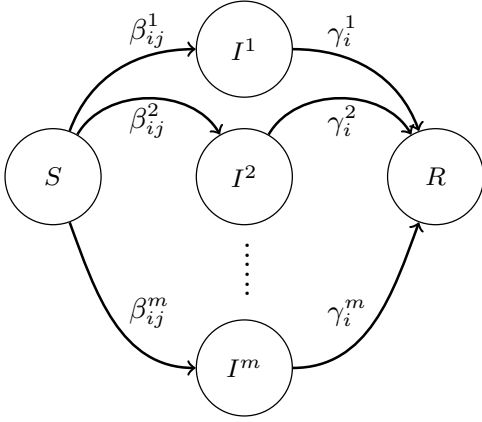


FIGURE 1: The competing SIR networked model. Each node in the network can only be in one of  $(m + 2)$  states:  $S$ ,  $I^k$ ,  $R$ , where  $k \in [m]$ .

$\rho(A)$  and  $\lambda(A)$ , respectively. A diagonal matrix is denoted by  $\text{diag}(\cdot)$ . The transpose of a vector  $x \in \mathbb{R}^n$  is  $x^\top$ . The Euclidean norm is denoted by  $\|\cdot\|$ . We use  $I$  to denote the identity matrix. We use  $\mathbf{0}$  and  $\mathbf{1}$  to denote the vectors whose entries are all 0 and 1, respectively, where the dimensions of the vectors are determined by context. Given a matrix  $A$ ,  $A \succ 0$  indicates that  $A$  is positive definite, whereas  $A \prec 0$  indicates that  $A$  is negative definite, and  $A^{-1}$  represents the inverse of matrix  $A$ . Let  $G = (\mathbb{V}, \mathbb{E})$  denote a graph or network where  $\mathbb{V} = \{v_1, v_2, \dots, v_n\}$  is the set of nodes, and  $\mathbb{E} \subseteq \mathbb{V} \times \mathbb{V}$  is the set of edges.

## II. BACKGROUND

In this section, we present our system model, recall some preliminary results that will be used in the sequel, and formally state the research questions that the paper addresses.

### A. System Model

Consider a network of  $n \geq 2$  nodes in which  $m$  ( $m \geq 2$ ), viruses compete to infect the nodes. A node here represents a well-mixed population (hereafter, referred to as a subpopulation) of individuals with a large and constant size. A node could be in one of  $m + 2$  mutually exclusive compartments: susceptible, infected with virus  $k$ ,  $k = [m]$ , or recovered. We say that a node is healthy if all individuals within it are healthy; otherwise, we say that it is infected. An individual in the susceptible compartment transitions to the "infected with virus  $k$ " (for  $k \in [m]$ ) compartment depending on its infection rate with respect to virus  $k$ , namely  $\beta_{ij}^k$ . An individual in the "infected with virus  $k$ " compartment transitions to the recovered compartment depending on its recovery rate with respect to virus  $k$ , namely  $\gamma_i^k$ .

We use an  $m$ -layer graph  $G$  to capture the spread of  $m$ -competing viruses. The vertices of  $G$  correspond to the population nodes. The contact graph that represents the pathways through which virus  $k$ , for each  $k \in [m]$ , spreads in the population is denoted by the  $k^{\text{th}}$  layer. In particular, there exists a directed edge from node  $j$  to node  $i$  in layer  $k$  if, assuming an individual in population  $j$  is infected with virus  $k$ , then said

individual can infect at least one healthy individual in node  $i$ . The edge set corresponding to the  $k^{\text{th}}$  layer of  $G$  is denoted by  $E^k$ , while  $A^k$  denotes the weighted adjacency matrix (where  $a_{ij}^k \geq 0$ ). Note that  $(i, j) \in E^k$  if, and only if,  $a_{ji}^k \neq 0$ . We denote by  $s_i$  and  $r_i$ , respectively, the susceptible and recovered proportions of subpopulation  $i$ . We use  $x_i^k[t]$ , where  $k \in [m]$ , to denote the fraction of individuals at node  $i$  infected with virus  $k$  at time instant  $t$ . A pictorial depiction of this model is given in Figure 1. In continuous time, the dynamics of the  $i$ -th node can be written as follows:

$$\dot{s}_i = -(1 - x_i^1 - \dots - x_i^m - r_i) \sum_{k=1}^m \sum_{j=1}^n \beta_{ij}^k x_j^k, \quad (1a)$$

$$\dot{x}_i^k = (1 - x_i^1 - \dots - x_i^m - r_i) \sum_{j=1}^n \beta_{ij}^k x_j^k - \gamma_i^k x_i^k, \quad (1b)$$

$$\dot{r}_i = \sum_{k=1}^m \gamma_i^k x_i^k, \quad \forall i \in [n]. \quad (1c)$$

Note that while an epidemic process evolves in continuous time, the data regarding the evolution of an epidemic are compiled on a daily basis [6], [50] or on a weekly basis [51]. Such a sampling of the system behavior motivates the use of a discrete-time multi-competitive networked SIR model. By using the Euler method [52], we derive the discrete-time dynamics of the SIR networked epidemic model at node  $i$  as:

$$s_i[t + 1] = s_i[t] - h \left( s_i[t] \sum_{k=1}^m \sum_{j=1}^n \beta_{ij}^k x_j^k[t] \right), \quad (2a)$$

$$x_i^k[t + 1] = x_i^k[t] + h \left( s_i[t] \sum_{j=1}^n \beta_{ij}^k x_j^k[t] - \gamma_i^k x_i^k[t] \right), \quad (2b)$$

$$r_i[t + 1] = r_i[t] + h \sum_{k=1}^m \gamma_i^k x_i^k[t], \quad (2c)$$

where  $h > 0$  is the sampling parameter,  $t$  is the time index, and  $k \in [m]$  indicates the  $k$ -th virus. Notice that  $s_i[t] + x_i^1[t] + \dots + x_i^m[t] + r_i[t] = 1$ , capturing the fact that in the competing virus scenario, all the viruses are mutually exclusive. We now rewrite (2b) in compact form as:

$$x^k[t + 1] = x^k[t] + h \{ S[t] B^k - \Gamma^k \} x^k[t], \quad (3)$$

where  $S[t] = \text{diag}(s_i[t])$ ,  $B^k$  is a matrix with  $(i, j)$ -th entry  $\beta_{ij}^k$ , and  $\Gamma^k[t] = \text{diag}(\gamma_i^k)$ .

We now introduce the following assumptions to ensure that the model in (2) is well-defined.

**Assumption 1.** For all  $i \in [n]$  and  $k \in [m]$ , we have  $s_i[0], x_i^k[0], r_i[0] \in [0, 1]$  and  $s_i[0] + \sum_{k=1}^m x_i^k[0] + r_i[0] = 1$ .

**Assumption 2.** For all  $i \in [n]$ , and  $k \in [m]$ , we have  $\beta_{ij}^k \geq 0, \gamma_i^k > 0$ .

**Assumption 3.** For all  $i \in [n]$ , and  $k \in [m]$ , we have  $h \sum_{k=1}^m \sum_{j=1}^n \beta_{ij}^k \leq 1$  and  $h \sum_{k=1}^m \gamma_i^k \leq 1$ .

Assumptions 1 and 2 can be interpreted as the initial proportion of susceptible, infected, and recovered individuals, all lying in the interval  $[0, 1]$ , and that the healing rates

are always positive, which are both reasonable [7], [33], [53]. Assumption 3 ensures that the sampling rate is frequent enough for the states of the model to remain well-defined.

Motivated by the fact that different infectious diseases can demonstrate similar symptoms over the hosts [44], [45], we build an observation model which produces the output as the aggregated proportion of individuals who show flu-like symptoms from infection of all viruses. The observation model is written as (where we repeat (2b) for convenience):

$$x_i^k[t+1] = x_i^k[t] + h \left\{ s_i[t] \sum_{j=1}^n \beta_{ij}^k x_j^k[t] - \gamma_i^k x_i^k[t] \right\}, \quad (4a)$$

$$y_i[t] = \sum_{k=1}^m c_i^k x_i^k[t], \quad (4b)$$

where  $c_i^k$  is the measurement coefficient.

**Assumption 4.** *The coefficient  $c_i^k \in (0, 1]$  for all  $i \in [n], k \in [m]$ .*

**Remark 1.** *The coefficient  $c_i^k$  from Eq. (4b) can capture the probability of showing symptoms from the  $k$ -th virus at subpopulation  $i$ . Therefore,  $1 - c_i^k$  captures the probability of individuals infected by the  $k$ -th virus in subpopulation  $i$  being asymptomatic. The probability of exhibiting symptoms corresponding to different viruses has been studied in, among others, [54], [55]. The coefficient  $c_i^k$  can also represent how each subpopulation  $i$  defines and measures the cases based on the symptoms of each virus  $k$ . For example, the symptoms of the SARS-CoV-2 virus can include but are not limited to fever, muscle aches, cough, runny nose, headaches, and fatigue.*

**Remark 2.** *Given a subpopulation  $i$ , Eq. (4b) captures the total proportion of symptomatic patients at subpopulation  $i$ . This value, namely  $y_i[t]$ , is a useful indicator for decision-makers to formulate policies regarding the adequacy of local healthcare facilities and the availability of virus-combating resources.*

We next present the following results for the system model under Assumptions 1-3.

**Lemma 1.** *Under Assumptions 1, 2, and 3, for all  $i \in [n]$  and  $t \in \mathbb{Z}_{\geq 0}$ ,*

- 1)  $s_i[t], x_i^k[t], r_i[t] \in [0, 1]$ , for all  $k \in [m]$ , and  $s_i[t] + \sum_{k=1}^m x_i^k[t] + r_i[t] = 1$ , and
- 2)  $s_i[t+1] \leq s_i[t]$ .

*Proof.* Proof of statement 1): We prove this result by induction.

*Base Case:* By the assumptions made,  $s_i[0], x_i^k[0], r_i[0] \in [0, 1]$ ,  $s_i[0] + \sum_{k=1}^m x_i^k[0] + r_i[0] = 1$  for all  $k \in [m], i \in [n]$ . From Assumptions 1-3, we know that  $s_i[0] \geq 0$  and  $1 - h \sum_k \sum_j \beta_{ij}^k x_j^k[0] \geq 0$ , and hence  $s_i[1] = s_i[0](1 - h \sum_k \sum_j \beta_{ij}^k x_j^k[0]) \geq 0$ . Since  $-h(s_i[t] \sum_k \sum_j \beta_{ij}^k x_j^k[0]) \leq 0$ , we obtain that  $s_i[1] \leq s_i[0] \leq 1$ . We can also acquire that  $x_i^k[1] \geq x_i^k[0](1 - h\gamma_i^k) \geq 0$  and  $x_i^k[1] \leq x_i^k[0] + h s_i[0] \sum_j \beta_{ij}^k x_j^k[0] \leq x_i^k[0] + s_i[0] \leq 1$ . Ultimately, we have  $r_i[1] \geq r_i[0] \geq 0$  and  $r_i[1] \leq r_i[0] + \sum_k x_i^k[0] \leq 1$ . Summing up Eqs. (2a)-(2c), we obtain that  $s_i[1] + \sum_{k=1}^m x_i^k[1] + r_i[1] = s_i[0] + \sum_{k=1}^m x_i^k[0] + r_i[0] = 1$ .

*Inductive Step:* We assume for some arbitrary  $t$  that the following holds:  $s_i[t], x_i^k[t], r_i[t] \in [0, 1]$ , for all  $k \in [m]$  and  $s_i[t] + \sum_{k=1}^m x_i^k[t] + r_i[t] = 1$ . By repeating the same steps from the *Base Case* except replacing 0 and 1 with  $k$  and  $k+1$ , we can write that  $s_i[t+1], x_i^k[t+1], r_i[t+1] \in [0, 1]$ , for all  $k \in [m]$  and  $s_i[t+1] + \sum_{k=1}^m x_i^k[t+1] + r_i[t+1] = 1$ . Therefore, by induction, we can prove that  $s_i[t], x_i^k[t], r_i[t] \in [0, 1]$ , for all  $k \in [m]$  and  $s_i[t] + \sum_{k=1}^m x_i^k[t] + r_i[t] = 1$  for all  $i \in [n]$  and  $t \in \mathbb{Z}_{\geq 0}$ .

Proof of statement 2): From 1) and Assumption 2 we know that  $-h \left( s_i[t] \sum_{k=1}^m \sum_{j=1}^n \beta_{ij}^k x_j^k[t] \right) \leq 0$  for all  $t \in \mathbb{Z}_{\geq 0}$ . Thus, we have  $s_i[t+1] \leq s_i[t]$  for all  $i \in [n]$  and  $t \in \mathbb{Z}_{\geq 0}$ .  $\square$

## B. Preliminaries

In this subsection, we recall certain preliminary results from non-linear systems theory that will help in the development of the main results of the paper.

Consider a system described as follows:

$$x[t+1] = f(t, x[t]), \quad (5a)$$

$$y[t] = g(x[t]). \quad (5b)$$

**Definition 1.** *An equilibrium point of (5a) is GES if there exist positive constants  $\alpha$  and  $\omega$ , with  $0 \leq \omega < 1$ , such that*

$$\|x[t]\| \leq \alpha \|x[t_0]\| \omega^{(t-t_0)}, \forall t \geq t_0 \geq 0, \forall x[t_0] \in \mathbb{R}^n. \quad (6)$$

**Lemma 2.** [56, Theorem 28] *Suppose that there exist a function  $V : \mathbb{Z}_+ \times \mathbb{R}^n \rightarrow \mathbb{R}$ , and constants  $a, b, c > 0$  and  $p > 1$  such that  $a\|x\|^p \leq V(t, x) \leq b\|x\|^p$ ,  $\Delta V(t, x) := V(x[t+1]) - V(x[t]) \leq -c\|x\|^p, \forall t \in \mathbb{Z}_{\geq 0}$ . Then  $\forall x(t_0) \in \mathbb{R}^n, x = \mathbf{0}$  is the globally exponential stable equilibrium of (5a).*

**Lemma 3.** [57, Theorem 23.3] *Under the conditions of Lemma 2, convergence to the origin has an exponential rate of at least  $\sqrt{1 - (c/b)} \in [0, 1)$ , where  $b$  and  $c$  are as defined in Lemma 2.*

**Lemma 4.** [58, Proposition 2] *Suppose that  $M$  is a nonnegative matrix which satisfies  $\rho(M) < 1$ . Then, there exists a diagonal matrix  $P \succ 0$  such that  $M^T P M - P \prec 0$ .*

**Definition 2.** *The system in Eq. (4) is strongly locally observable at  $s[t]$  if we are able to recover  $x_i^k[t]$  for all  $i \in [n], k \in [m]$  through the output in the duration of  $[t, t+m-1]$ .*

**Lemma 5.** [59], [60] *The system in (5) is strongly locally observable at  $x[t]$  if and only if the map  $x[t] \rightarrow (g(x[t]), g(f^1(x[t])), \dots, g(f^{n-1}(x[t])))$  is injective, where  $n$  is the dimension of  $x[t]$ .*

## C. Problem Formulation

With the system model set up as above, we now introduce the problems investigated in this paper.

- (i) For the system with dynamics given in (3), provide a sufficient condition which ensures that  $x^k[t]$  for some  $k \in$

$[m]$  converges to the eradicated state, namely  $x^k = \mathbf{0}$ , in exponential time.

- (ii) What is the rate of convergence for the sequence  $x^k[t]$ ,  $k \in [m]$  (converging to  $\mathbf{0}$  exponentially)?
- (iii) Provided that the infection rate matrix  $B^k$ , healing rate matrix  $\Gamma^k$ , the observation  $y_i[t]$ , true susceptible states  $s_i[t]$ , and the measurement coefficient  $c_i^k$ , are known, for all  $i \in [n]$ ,  $k \in [m]$ , under what conditions are the infection levels of each virus  $x_i^k[t]$ , for all  $i \in [n]$ ,  $k \in [m]$  strongly locally observable, at  $s_i[t] = 0, \forall i \in [n]$ ?
- (iv) Given the system parameters  $\beta_{ij}^k, \gamma_i^k$  for all  $i, j \in [n]$ ,  $k \in [m]$ , and the local aggregated observation,  $y_i[t]$  for all  $i \in [n]$ , construct a distributed Luenberger observer which delivers the system states  $\hat{s}_i[t], \hat{x}_i^k[t], \hat{r}_i[t]$  for all  $i \in [n]$ ,  $k \in [m]$ ?
- (v) Given the system parameters  $\beta_{ij}^k, \gamma_i^k$  for all  $i, j \in [n]$ ,  $k \in [m]$ , how do we find the gain of the distributed observer such that the estimation error  $x^k[t] - \hat{x}^k[t]$  converges to zero asymptotically for all  $k \in [m]$ ?
- (vi) Design a distributed feedback controller which eradicates all viruses at an exponential rate.

### III. HEALTHY STATE ANALYSIS

In this section, we identify multiple sufficient conditions which guarantee that each virus  $k$  converges to zero exponentially fast, and provide the associated rates of convergence for each virus. Similar to the standard single virus SIR networked model, the multi-competitive SIR networked model also converges to a healthy state regardless of i) the values that the system parameters take, and ii) initial conditions. However, it is important to study the exponential convergence since it guarantees that the viruses die out at a faster rate and, as a consequence, fewer individuals become infected over the course of the outbreak [31].

Let

$$M^k := I - h\Gamma^k + hB^k, \quad (7)$$

$$\tilde{M}^k[t] := I + h\{S[t]B^k - \Gamma^k\}, \quad (8)$$

and note that  $\tilde{M}^k$  is the state matrix of system (3):

$$\tilde{M}^k[t] = M^k - h(I - S[t])B^k. \quad (9)$$

We first present a sufficient condition, in terms of  $M^k$ , for the infection level with respect to each of the viruses to converge to zero exponentially.

**Theorem 1.** *Consider system (2) under Assumptions 1-3. If  $\rho(M^k) < 1$ , then the  $k$ -th virus of the system in (2) converges to zero in exponential time.*

The proof of Theorem 1 is inspired by the proof of [61, Theorem 1].

*Proof:* Consider an arbitrary virus  $k \in [m]$ . By Assumptions 2 and 3,  $M^k$ , defined by Eq. (7), is nonnegative for all  $k \in [m]$ , and from the condition we know that  $\rho(M^k) < 1$ . Therefore, according to Lemma 4, for each  $k \in [m]$ , there exists a positive definite diagonal matrix  $P^k$  such that  $(M^k)^\top P^k M^k - P^k$  is negative definite.

Consider the candidate Lyapunov function:  $V_1^k(t, x^k) = (x^k)^\top P^k x^k$ . Since  $P^k$  is diagonal and positive definite,  $(x^k)^\top P^k x^k > 0$ , for all  $x^k \neq \mathbf{0}$ . Therefore,  $V_1^k(t, x^k) > 0$  for all  $k \in [m], t \in \mathbb{Z}_{\geq 0}, x^k \neq \mathbf{0}$ . Since  $P^k$  is positive definite,

$$\lambda_{\min}(P^k)I \leq P^k \leq \lambda_{\max}(P^k)I, \quad (10)$$

which implies that

$$\sigma_1^k \|x^k\|^2 \leq V_1^k(t, x^k) \leq \sigma_2^k \|x^k\|^2, \quad (11)$$

where  $\sigma_1^k = \lambda_{\min}(P^k)$  and  $\sigma_2^k = \lambda_{\max}(P^k)$ , with  $\sigma_1^k, \sigma_2^k > 0$ .

Now we turn to computing  $\Delta V_1^k(t, x^k)$ . For  $x^k \neq \mathbf{0}$  and for all  $k \in [m]$ , using (3) and (7)-(8), we have

$$\begin{aligned} \Delta V_1^k(t, x^k) &= (x^k)^\top \tilde{M}^k[t]^\top P^k \tilde{M}^k[t] x^k - (x^k)^\top P^k x^k \\ &= (x^k)^\top [(M^k)^\top P^k M^k - P^k] x^k \\ &\quad - 2h(x^k)^\top (B^k)^\top (I - S[t]) P^k M^k x^k \\ &\quad + h^2(x^k)^\top (B^k)^\top (I - S[t]) P^k (I - S[t]) B^k x^k. \end{aligned} \quad (12)$$

Note that the second and third terms of (12) can be reorganized as

$$\begin{aligned} &(x^k)^\top [-2h(B^k)^\top (I - S[t]) P^k M^k \\ &\quad + h^2(B^k)^\top (I - S[t]) P^k (I - S[t]) B^k] x^k \\ &= (x^k)^\top \{h(B^k)^\top (I - S[t]) P^k \\ &\quad [-2M^k + h(I - S[t]) B^k]\} x^k \\ &= (x^k)^\top \{h(B^k)^\top (I - S[t]) P^k \\ &\quad [-2(I - h\Gamma^k[t]) - h(I + S[t]) B^k]\} x^k \leq 0, \end{aligned} \quad (13)$$

where the last equality follows from (7), and the inequality follows from Assumptions 2-3 and Lemma 1. Thus, by plugging (13) into (12), we obtain

$$\Delta V_1^k(t, x^k) \leq (x^k)^\top [(M^k)^\top P^k M^k - P^k] x^k. \quad (14)$$

Since  $[(M^k)^\top P^k M^k - P^k]$  is negative definite, we have, from Eq. (14),

$$\Delta V_1^k(t, x^k) \leq -\sigma_3^k \|x^k\|^2, \quad (15)$$

where  $\sigma_3^k = \lambda_{\min}[P^k - (M^k)^\top P^k M^k]$ , with  $\sigma_3^k > 0$ .

Therefore, from (11) and (15),  $V_1^k(t, x^k)$  is a Lyapunov function with exponential decay, and, hence,  $x^k$  converges to zero at an exponential rate.  $\square$

**Corollary 1.** *Suppose that the conditions in Theorem 1 are fulfilled, and that  $P^k$  is as defined in the proof of Theorem 1. Then the convergence of  $x^k[t]$  has an exponential rate of at least  $\sqrt{1 - \frac{\sigma_3^k}{\sigma_2^k}}$ , where  $\sigma_2^k = \lambda_{\max}(P^k)$ ,  $\sigma_3^k = \lambda_{\min}[P^k - (M^k)^\top P^k M^k]$  for each  $k \in [m]$ .*

*Proof:* From Lemma 3, (11), and (15), the rate of convergence of virus  $k$  is upper-bounded by  $\sqrt{1 - \frac{\sigma_3^k}{\sigma_2^k}}$ . We then need to show that the rate is well-defined, which is  $\sqrt{1 - \frac{\sigma_3^k}{\sigma_2^k}} \in [0, 1)$ . Since  $\sigma_2^k > 0$  and  $\sigma_3^k > 0$ , it will be sufficient to show that  $\sigma_2^k \geq \sigma_3^k$ .

Since  $P^k$  is positive definite and  $(M^k)^\top P^k M^k$  is nonnegative definite, we have

$$\sigma_3^k I \leq P^k - (M^k)^\top P^k M^k \leq P^k \leq \sigma_2^k I, \quad (16)$$

from which  $\sigma_2^k \geq \sigma_3^k$  and the rate of convergence  $\sqrt{1 - \frac{\sigma_3^k}{\sigma_2^k}}$  is well-defined.  $\square$

In words, Theorem 1 says that if the state matrix corresponding to system (3), linearized around  $s_i = 1$  for  $i \in [n]$ , is Schur, then virus  $k$ , irrespective of its initial infection levels in the population, becomes extinct exponentially fast.

We now present another sufficient condition, which depends on the spectral radius of  $\tilde{M}^k[t]$ , for the infection level with respect to each of the viruses to converge to zero at an exponential rate.

**Proposition 1.** *Consider the system in (2) under Assumptions 1-3. If  $\rho(\tilde{M}^k[t]) < 1$  for all  $t \in \mathbb{Z}_{\geq 0}$ , then the  $k$ -th virus of the system in (2) converges to zero in exponential time, with at least an exponential rate of  $\min_{\forall t \in \mathbb{Z}_{\geq 0}} [1 - \rho(\tilde{M}^k[t])]$ .*

*Proof.* Define  $\epsilon^k[t] := 1 - \rho(\tilde{M}^k[t])$ . Hence, we obtain that  $\epsilon^k[t] > 0$  for all  $k \in [m]$  and  $t \in \mathbb{Z}_{\geq 0}$ . Since we have  $x^k[t+1] = \tilde{M}^k[t]x^k[t]$  and  $x^k[t] \geq 0$  for all  $t \in \mathbb{Z}_{\geq 0}$ , we can write that

$$\frac{\|x^k[t+1]\|}{\|x^k[t]\|} = \frac{\|\tilde{M}^k[t]x^k[t]\|}{\|x^k[t]\|} = |\lambda(\tilde{M}^k[t])| \leq \rho(\tilde{M}^k[t]), \quad (17)$$

which results in  $\|x^k[t+1]\| \leq (1 - \epsilon^k[t])\|x^k[t]\|$  for all  $t$ . Recall that,  $\epsilon^k[t] > 0$  for all  $k \in [m]$  and  $t \in \mathbb{Z}_{\geq 0}$ . Then, we obtain that, for all  $x_i^k[0] \in [0, 1]^n$ ,

$$\|x^k[t]\| \leq [1 - \min_{\forall t \in \mathbb{Z}_{\geq 0}} \epsilon^k[t]]^t \|x^k[0]\| \leq e^{-t \min_{\forall t \in \mathbb{Z}_{\geq 0}} \epsilon^k[t]} \|x^k[0]\|,$$

where the second inequality is due to Bernoulli's inequality [62]. Hence,  $x^k[t]$  converges to  $\mathbf{0}$  with at least an exponential rate of  $\min_{\forall t \in \mathbb{Z}_{\geq 0}} \epsilon^k[t]$ .  $\square$

Note that  $\rho(M^k)$  is the basic reproduction number of virus  $k$ , the average number of infections produced by an infected individual in a population where everyone is susceptible, and  $\rho(\tilde{M}^k[t])$  is the effective reproduction number of virus  $k$  over the network, the average number of infected cases caused by an infected individual in a population made up of both susceptible and non-susceptible individuals. It can be seen that Theorem 1 is a stronger global exponential stability condition than Proposition 1, as  $M^k$  is the linearized state transition matrix for virus  $k$  which does not depend on the susceptible state. However, Proposition 1 is important in its own right, since it provides insights into the design of a feedback controller; see Section V.

#### IV. STATE OBSERVATION MODEL

In this section, we analyze the observation model introduced in Eq. (4a) and Eq. (4b). In particular, we focus on identifying conditions guaranteeing strong local observability of our proposed system model around  $s_i[t] = 0$ , and on estimating the system states with respect to each virus.

As a first step, we construct the observability matrix for the system by writing Eq. (4b) as:

$$\mathbf{y}[t] = \mathbf{C}\mathbf{X}[t], \quad (18)$$

where  $\mathbf{y}[t] = [y_1[t] \ y_2[t] \ \dots \ y_n[t]]^\top \in \mathbb{R}^n$ ; the measurement matrix  $\mathbf{C} \in \mathbb{R}^{n \times mn}$  is defined as:

$$\mathbf{C} = [C^1 \ C^2 \ \dots \ C^m]$$

with  $C^k = \text{diag}([c_1^k, c_2^k, \dots, c_n^k])$  for all  $k \in [m]$ ; and

$$\mathbf{X}[t] = [x^1[t]^\top \ x^2[t]^\top \ \dots \ x^m[t]^\top]^\top.$$

Therefore, the measurement  $\mathbf{y}[t]$  can be reorganized as:

$$\mathbf{y}[t] = C^1 x^1[t] + C^2 x^2[t] + \dots + C^m x^m[t]. \quad (19)$$

The measurements, corresponding to each time step, over a time horizon  $[t, t+m-1]$  can be concatenated in a vector as follows:

$$\begin{aligned} & \begin{bmatrix} \mathbf{y}[t] \\ \mathbf{y}[t+1] \\ \mathbf{y}[t+2] \\ \vdots \\ \mathbf{y}[t+m-1] \end{bmatrix} \\ &= \begin{bmatrix} C^1 x^1[t] + \dots + C^m x^m[t] \\ C^1 x^1[t+1] + \dots + C^m x^m[t+1] \\ C^1 x^1[t+2] + \dots + C^m x^m[t+2] \\ \vdots \\ C^1 x^1[t+m-1] + \dots + C^m x^m[t+m-1] \end{bmatrix} \\ &= \begin{bmatrix} C^1 \\ C^1 \tilde{M}^1[t] \\ C^1 \tilde{M}^1[t] \tilde{M}^1[t+1] \\ \vdots \\ C^1 \tilde{M}^1[t] \dots \tilde{M}^1[t+m-2] \end{bmatrix} x^1[t] \\ &+ \begin{bmatrix} C^2 \\ C^2 \tilde{M}^2[t] \\ C^2 \tilde{M}^2[t] \tilde{M}^2[t+1] \\ \vdots \\ C^2 \tilde{M}^2[t] \dots \tilde{M}^2[t+m-2] \end{bmatrix} x^2[t] + \dots \\ &+ \begin{bmatrix} C^m \\ C^m \tilde{M}^m[t] \\ C^m \tilde{M}^m[t] \tilde{M}^m[t+1] \\ \vdots \\ C^m \tilde{M}^m[t] \dots \tilde{M}^m[t+m-2] \end{bmatrix} x^m[t] \\ &= \mathcal{O}^1[t] x^1[t] + \mathcal{O}^2[t] x^2[t] + \dots + \mathcal{O}^m[t] x^m[t] \\ &= [\mathcal{O}^1[t] \ \mathcal{O}^2[t] \ \dots \ \mathcal{O}^m[t]] \mathbf{X}[t], \quad (20) \end{aligned}$$

where the matrix  $\tilde{M}^k[t]$  is as defined in Eq. (8), and

$$\mathcal{O}^k[t] = \begin{bmatrix} C^k \\ C^k \tilde{M}^k[t] \\ C^k \tilde{M}^k[t] \tilde{M}^k[t+1] \\ \vdots \\ C^k \tilde{M}^k[t] \dots \tilde{M}^k[t+m-2] \end{bmatrix},$$

with  $\mathcal{O}^k[t] \in \mathbb{R}^{mn \times n}$  for all  $k \in [m]$ . We define the observability matrix of the system in Eq. (4) as:

$$\mathbb{O}[t] = [\mathcal{O}^1[t] \quad \mathcal{O}^2[t] \quad \cdots \quad \mathcal{O}^m[t]], \quad (21)$$

where  $\mathbb{O}[t] \in \mathbb{R}^{mn \times mn}$ .

We are interested in identifying a sufficient condition for strong local observability of our model when the network consists only of infected and/or recovered individuals; in other words, there are no susceptible individuals in any of the population nodes. Hence, we consider the case when  $s_i[t] = 0, \forall i \in [n]$ . Then the observability matrix in Eq. (21) becomes

$$\mathbb{O}_0[t] = [\mathcal{O}_0^1[t] \quad \mathcal{O}_0^2[t] \quad \cdots \quad \mathcal{O}_0^m[t]], \quad (22)$$

where

$$\mathcal{O}_0^k[t] = \begin{bmatrix} C^k \\ C^k(I - h\Gamma^k) \\ C^k(I - h\Gamma^k)^2 \\ \vdots \\ C^k(I - h\Gamma^k)^{m-1} \end{bmatrix}, \quad (23)$$

for all  $k \in [m]$ .

We have the following result.

**Theorem 2.** *Consider the system in Eq. (4) under Assumptions 1-4. Suppose that  $y_i(t)$ , for all  $i \in [n]$  and  $t \in [t, t + m - 1]$  is known. If, for each  $i \in [n]$ ,  $\gamma_i^k \neq \gamma_i^{k_0}$  for all  $k, k_0 \in [m]$  and  $k \neq k_0$ , then the system in Eq. (4) is strongly locally observable at  $s_i(t) = 0$  for all  $i \in [n]$ .*

*Proof.* From the assumptions  $h \sum_{k=1}^m \gamma_i^k \leq 1$ ,  $h > 0$ , and  $\gamma_i^k > 0$  for all  $i \in [n], k \in [m]$ , we obtain that  $1 - h\gamma_i^k \in (0, 1)$  for all  $i \in [n], k \in [m]$ . In addition, by Assumption 4,  $c_i^k \in (0, 1)$  for all  $i \in [n], k \in [m]$ , we can conclude that the entries of Eq. (22):  $c_i^k(1 - h\gamma_i^k) \in (0, 1)$  for all  $i \in [n], k \in [m]$ .

We let  $\mathbf{0}^n := [0 \quad 0 \quad \cdots \quad 0]^{1 \times n}$  and  $\mathbf{0}^0 := \emptyset$ . Consider Eq. (23) and recall that every block matrix is diagonal; hence, Eq. (22) is the concatenation of a set of block diagonal matrices. For all  $i \in [n]$ , the  $i$ -th row of the observability matrix (22) can be written as:

$$[\mathbf{0}^{i-1} \quad c_i^1 \quad \mathbf{0}^{n-i} \quad \mathbf{0}^{i-1} \quad c_i^2 \quad \mathbf{0}^{n-i} \quad \cdots \quad \mathbf{0}^{i-1} \quad c_i^m \quad \mathbf{0}^{n-i}]$$

which is linearly independent with the  $(i + ln)$ -th row of (22) for all  $l \in [m - 1]$ :

$$[\mathbf{0}^{i-1} \quad c_i^1(1 - h\gamma_i^1)^l \quad \mathbf{0}^{n-i} \quad \cdots \quad \mathbf{0}^{i-1} \quad c_i^m(1 - h\gamma_i^m)^l \quad \mathbf{0}^{n-i}]$$

under our assumption that, for each  $i \in [n]$ ,  $\gamma_i^k \neq \gamma_i^{k_0}$  for all  $k, k_0 \in [m]$  and  $k \neq k_0$ . Thus, the observability matrix in Eq. (22) has full row rank. Since the observability matrix is a square matrix, we conclude that the observability matrix,  $\mathbb{O}_0[t]$ , is full rank. Therefore, the mapping in Eq. (20) when  $s_i[t] = 0, \forall i \in [n]$  is injective. Note that  $mn$  is the dimension of  $\mathbf{X}[t]$ . Hence, by Lemma 5, the competing virus model in (4) is strongly locally observable at  $s_i[t] = 0, \forall i \in [n]$ .  $\square$

Notice that whenever we add another virus to our model (4), we increase the dimension of (22) from  $mn \times mn$  to  $(m + 1)n \times (m + 1)n$ , and, due to the same reasons as in the proof of Theorem 2, the rank of the observability matrix will be  $(m + 1)n$ .

**Remark 3.** *The assumption in Theorem 2, namely that, for each  $i \in [n]$ ,  $\gamma_i^k$  is a distinct value across every  $k \in [m]$ , can be interpreted as each node's recovery rates with respect to every virus are distinct. This assumption is reasonable as the recovery rate represents the inverse of the average duration of an infected individual to be sick, and the average amount of time for an individual to recover from different types/strains of viruses varies drastically [63].*

Theorem 2 provides a sufficient condition for strong local observability when the fraction of susceptible population in each node is zero. Note that this condition identifies a scenario that admits the design of an observer for estimating the system states, but it does not say *how* the states of the system can be estimated. Hence, in the sequel, we focus on the estimation of the system states.

The dynamics of the estimated states are

$$\hat{x}_i^k[t + 1] = \hat{x}_i^k[t] + h \left\{ \hat{s}_i[t] \sum_{j=1}^n \beta_{ij}^k \hat{x}_j^k[t] - \gamma_i^k \hat{x}_i^k[t] \right\}, \quad (24)$$

$$\hat{y}_i[t + 1] = \sum_{k=1}^m c_i^k \hat{x}_i^k[t + 1], \quad (25)$$

where

$$\hat{s}_i[t] = 1 - \sum_{k=1}^m \hat{x}_i^k[t] - \hat{r}_i[t] \quad (26)$$

and the recovered level is estimated by:

$$\hat{r}_i[t] = h \sum_{q=0}^t \sum_{k=1}^m \gamma_i^k \hat{x}_i^k[q] \quad (27)$$

at each time step, recursively. Notice that in Eq. (24), in order to acquire the estimated infection level at node  $i$ , we need some knowledge of the infection levels from all the neighbors of node  $i$ , namely  $\hat{x}_j^k[t]$  for all  $\beta_{ij}^k \neq 0$ . Hence, we have the following definition and assumption.

**Definition 3.** *For node  $j$ , which is a neighbor node of node  $i$ , namely  $\beta_{ij}^k > 0$ , we define the estimated infection level at node  $j$  acquired by node  $i$  at time  $t$  as  $\hat{x}_j^k[t - \mathcal{T}_j] + \mathcal{E}_j$ , where  $\mathcal{T}_j \in \mathbb{Z}_{\geq 0}$  is the time delay between nodes  $i$  and  $j$ , and  $\mathcal{E}_j \in \mathbb{R}$  is the reporting error at node  $j$ .*

**Assumption 5.** *For the estimation algorithm, the nodes share their estimated infection levels with no time delay or error, namely  $\mathcal{T}_j = 0, \mathcal{E}_j = 0$  for all  $j \in [n]$  in Definition 3.*

Through Assumption 5, we have that every node in the network is completely cooperative and honest to its neighboring nodes. Hence, under Assumption 5, our proposed distributed Luenberger observer is:

$$\begin{aligned} \hat{x}_i^k[t + 1] = & \hat{x}_i^k[t] + h \left\{ \hat{s}_i[t] \sum_{j=1}^n \beta_{ij}^k \hat{x}_j^k[t] - \gamma_i^k \hat{x}_i^k[t] \right\} \\ & + L_i^k (y_i[t] - \hat{y}_i[t]), \end{aligned} \quad (28)$$

where  $L_i^k$  is the observer gain which, given a node  $i$ , can be chosen for each  $k \in [m]$ . We can write  $e_i^k[t] = x_i^k[t] -$

$\hat{x}_i^k[t]$  as the error of the observer. Hence, the dynamics of the estimation error are written as:

$$\begin{aligned}
e_i^k[t+1] &= x_i^k[t+1] - \hat{x}_i^k[t+1] \\
&= (1 - h\gamma_i^k)e_i^k[t] + h \sum_{j=1}^n \beta_{ij}^k e_j^k[t] - L_i^k \sum_{k=1}^m c_i^k e_i^k[t] \\
&\quad - h \left( \sum_{k=1}^m x_i^k[t] \sum_{j=1}^n \beta_{ij}^k x_j^k[t] - \sum_{k=1}^m \hat{x}_i^k[t] \sum_{j=1}^n \beta_{ij}^k \hat{x}_j^k[t] \right) \\
&\quad - h \left( \sum_q^t \sum_{k=1}^m \gamma_i^k x_i^k[q] \sum_{j=1}^n \beta_{ij}^k x_j^k[q] \right. \\
&\quad \left. - \sum_q^t \sum_{k=1}^m \gamma_i^k \hat{x}_i^k[q] \sum_{j=1}^n \beta_{ij}^k \hat{x}_j^k[q] \right). \tag{29}
\end{aligned}$$

We then rewrite the error dynamics (29) as:

$$e^k[t+1] = (M^k - L^k C^k)e^k[t] + w^k[t] \tag{30}$$

where recall that

$$M^k = I - h\Gamma^k + hB^k$$

and

$$\begin{aligned}
w^k[t] &= -L^k \sum_{p \neq k}^m c^p e^p[t] \\
&\quad + h \left\{ \left( \sum_{k=1}^m x^k[t] \right) B^k x^k[t] - \left( \sum_{k=1}^m \hat{x}^k[t] \right) B^k \hat{x}^k[t] \right\} \\
&\quad + h \left\{ \sum_q^t \sum_{k=1}^m \Gamma^k x^k[q] B^k x^k[q] - \sum_q^t \sum_{k=1}^m \gamma_i^k \hat{x}_i^k[q] B^k \hat{x}^k[q] \right\} \tag{31}
\end{aligned}$$

with  $L^k = \text{diag}(L_i^k)$ .

Inspired by [46], we aim to show that the estimation error of our Luenberger observer (28) converges to zero asymptotically. We make the following assumption.

**Assumption 6.** *There exists a constant  $l^k$  for each virus  $k \in [m]$  such that:*

$$\|w^k[t]\| \leq l^k \|x^k[t] - \hat{x}^k[t]\| \tag{32}$$

for all  $t \in \mathbb{Z}_{\geq 0}$ .

**Corollary 2.** *For each  $k \in [m]$ , inequality (32) can be rewritten as:*

$$l^k \geq \frac{\|w^k[t]\|}{\|x^k[t] - \hat{x}^k[t]\|} \tag{33}$$

for all  $t \in \mathbb{Z}_{\geq 0}$ .

Note that, in many cases, we are able to tune the observer gain  $L^k$  to satisfy the inequality (32) in Assumption 6. We explore the feasibility of Assumption 6 via simulations in Section VI.

We now identify a sufficient condition with respect to the observer gain, which guarantees that the estimation errors converge to zero asymptotically.

**Theorem 3.** *Under Assumption 6, the estimation error of the Luenberger observer (28) for virus  $k$  converges to zero*

*asymptotically if there exist a symmetric matrix  $Q^k \succ 0$  and  $\tau^k \in (0, 1]$  such that the following inequalities are satisfied:*

$$\begin{aligned}
&(M^k - L^k C^k)^\top [Q^k - (Q^k)^\top (Q^k - \tau^k I)^{-1} Q^k] (M^k - L^k C^k) \\
&\quad - Q^k + \tau^k (l^k)^2 I \prec 0 \tag{34}
\end{aligned}$$

and

$$Q^k - \tau^k I \prec 0. \tag{35}$$

where  $L^k$  is the observer gain for virus  $k$ .

*Proof.* From Assumption 6, we can write that

$$(w^k[t])^\top w^k[t] \leq (l^k)^2 (e^k[t])^\top e^k[t]$$

which can be rewritten as

$$[(e^k[t])^\top \quad (w^k[t])^\top] \Phi^k \begin{bmatrix} e^k[t] \\ w^k[t] \end{bmatrix} \leq 0, \tag{36}$$

where

$$\Phi^k = \begin{bmatrix} -(l^k)^2 I & 0 \\ 0 & I \end{bmatrix}.$$

By utilizing the Schur complement [64], and defining  $A^k = (M^k - L^k C^k)^\top Q^k (M^k - L^k C^k)$ , where  $Q^k$  is a symmetric positive definite matrix by assumption, we can reorganize Eqs. (34) and (35) as

$$\begin{bmatrix} A^k - Q^k + \tau^k (l^k)^2 I & (M^k - L^k C^k)^\top Q^k \\ Q^k (M^k - L^k C^k) & Q^k - \tau^k I \end{bmatrix} \prec 0, \tag{37}$$

which yields the following:

$$\Omega^k - \tau^k \Phi^k \prec 0, \tag{38}$$

where

$$\Omega^k = \begin{bmatrix} A^k - Q^k & (M^k - L^k C^k)^\top Q^k \\ Q^k (M^k - L^k C^k) & Q^k \end{bmatrix}.$$

We now consider the candidate Lyapunov function  $V_2^k(e^k, [t]) = (e^k[t])^\top Q^k (e^k[t])$ , where  $Q^k$  is the positive definite matrix in (37). We can write that

$$V_2^k(e^k, [t]) > 0, \text{ for all } e^k[t] \neq 0$$



and

$$\begin{aligned}
& \Delta V_2^k \\
&= V_2^k(e^k[t+1], t) - V_2^k(e^k[t], t) \\
&= \left[ (M^k - L^k C^k) e^k[t] + w^k[t] \right]^\top Q^k \\
&\quad \left[ (M^k - L^k C^k) e^k[t] + w^k[t] \right] - (e^k[t])^\top Q^k e^k[t] \\
&= (e^k[t])^\top A^k e^k[t] \\
&\quad + (w^k[t])^\top Q^k (M^k - L^k C^k) e^k[t] \\
&\quad + (e^k[t])^\top (M^k - L^k C^k)^\top Q^k w^k[t] + (w^k[t])^\top Q^k w^k[t] \\
&\quad - (e^k[t])^\top Q^k e^k[t] \\
&= (e^k[t])^\top (A^k - Q^k) e^k[t] \\
&\quad + (w^k[t])^\top Q^k (M^k - L^k C^k) e^k[t] \\
&\quad + (e^k[t])^\top (M^k - L^k C^k)^\top Q^k w^k[t] \\
&\quad + (w^k[t])^\top Q^k w^k[t] \\
&= \begin{bmatrix} (e^k[t])^\top & (w^k[t])^\top \end{bmatrix} \Omega^k \begin{bmatrix} e^k[t] \\ w^k[t] \end{bmatrix} \\
&< \begin{bmatrix} (e^k[t])^\top & (w^k[t])^\top \end{bmatrix} \tau^k \Phi^k \begin{bmatrix} e^k[t] \\ w^k[t] \end{bmatrix} \tag{39} \\
&\leq 0, \tag{40}
\end{aligned}$$

where inequality (39) follows from (38), and inequality (40) follows from inequality (36). Therefore, by Lyapunov's direct method [56], the estimation error of the Luenberger observer (28) for virus  $k$  is globally asymptotically stable.  $\square$

**Remark 4.** Note that we need the pair  $(M^k, C^k)$  to be detectable for inequalities (34) and (35) to hold [46], [47]. Under Assumption 4, the pair  $(M^k, C^k)$  is observable, and, thus, detectable.

**Corollary 3.** The inequalities (34) and (35) combined together in Theorem 3 are equivalent to the following LMI:

$$\begin{bmatrix} -Q^k + \tau^k (L^k)^2 I & (M^k)^\top Q^k - (C^k)^\top R^k & (M^k)^\top Q^k - (C^k)^\top R^k \\ \begin{bmatrix} (M^k)^\top Q^k - (C^k)^\top R^k \\ (M^k)^\top Q^k - (C^k)^\top R^k \end{bmatrix}^\top & Q^k - \tau^k I & \mathbf{0} \\ \begin{bmatrix} (M^k)^\top Q^k - (C^k)^\top R^k \\ (M^k)^\top Q^k - (C^k)^\top R^k \end{bmatrix}^\top & \mathbf{0} & -Q^k \end{bmatrix} < 0 \tag{41}$$

where  $(R^k)^\top = Q^k L^k$ .

By applying Schur complement, LMI (41) can be shown to be equivalent to Eq. (37) and  $-Q^k \prec 0$ . Note that LMI (41) can be solved through the *cvx* solver in MATLAB for simulations.

## V. DISTRIBUTED FEEDBACK CONTROL

In this section, we present a distributed feedback mitigation strategy for ensuring that all viruses are eradicated. We establish that virus  $k$  can be eradicated in exponential time by boosting the healing rate associated with virus  $k$ . Applying such eradication strategy for all  $m$  viruses, the system converges to a healthy state.

When battling against the spread of an epidemic, boosting the healing rate with respect to the virus is a common

approach [31], [61]. Boosting the healing rates could be implemented by means of providing effective medication, medical supplies, and/or healthcare workers to each subpopulation.

The key tool behind devising the aforementioned mitigation strategy is Proposition 1, which says that if the spectral radius of the state transition matrix of virus 1 is less than one, i.e.,  $\rho(\tilde{M}^k[t]) < 1$ , then the infection level of the  $k$ -th virus converges to zero within at least exponential time. Accordingly, we formally state our distributed feedback control strategy as follows:

$$\tilde{\gamma}_i^k[t] = \gamma_i^k - u_i^k[t], \quad i \in [n], \tag{42}$$

where  $u_i^k[t]$  is a state feedback controller, with

$$\begin{aligned}
u_i^k[t] &= -s_i[t] \sum_{j=1}^n \beta_{ij}^k \\
&= -\left(1 - \sum_{k=1}^m x_i^k[t] - r_i[t]\right) \sum_{j=1}^n \beta_{ij}^k. \tag{43}
\end{aligned}$$

We have the following result.

**Theorem 4.** Consider the system in (2), under Assumptions 2 and 3, and assume further that  $h\tilde{\gamma}_i^k[t] < 1$ ,  $\forall i \in [n], t \in \mathbb{Z}_{\geq 0}$ . Then the feedback controller in Eq. (42) guarantees that virus  $k$  is eradicated with at least an exponential rate of  $h \min_{i \in [n]} \{\gamma_i^k\}$ .

*Proof.* By substituting Eq. (42) and Eq. (43) into (2b), we obtain

$$\begin{aligned}
x_i^k[t+1] &= x_i^k[t] + \\
&h \left\{ s_i[t] \sum_{j=1}^n \beta_{ij}^k x_j^k[t] - \left[ s_i[t] \sum_{j=1}^n \beta_{ij}^k + \gamma_i^k \right] x_i^k[t] \right\}. \tag{44}
\end{aligned}$$

The state transition matrix of (44) can be written as

$$\tilde{M}^k[t] = I + h \left[ S[t] B^k - (S[t] \text{diag}(B^k \mathbf{1}_{n \times 1}) + \text{diag}(\gamma_i^k)) \right].$$

The entries of the  $i$ -th row of  $\tilde{M}^k[t]$ , therefore, are

$$\begin{aligned}
\tilde{m}_{ii}^k[t] &= 1 + h \left[ s_i[t] \beta_{ii}^k - s_i[t] \sum_{j=1}^n \beta_{ij}^k - \gamma_i^k \right], \\
\tilde{m}_{ij}^k[t] &= h s_i[t] \beta_{ij}^k,
\end{aligned}$$

which satisfies the following inequality

$$\tilde{m}_{ii}^k[t] + \sum_{j \neq i} \tilde{m}_{ij}^k[t] \leq 1 - \gamma_i^k, \quad \forall i \in n.$$

Therefore, by Gershgorin circle theorem, the spectral radius of  $\tilde{M}^k[t]$  is upper bounded by  $1 - h \min_{i \in [n]} \{\gamma_i^k\}$ , that is,

$$\rho(\tilde{M}^k[t]) \leq 1 - h \min_{i \in [n]} \{\gamma_i^k\}.$$

Since we have  $x^k[t+1] = \tilde{M}^k[t] x^k[t]$  and  $x^k[t] \geq 0$  for all  $t \in \mathbb{Z}_{\geq 0}$ , we can write that

$$\frac{\|x^k[t+1]\|}{\|x^k[t]\|} = \frac{\|\tilde{M}^k[t] x^k[t]\|}{\|x^k[t]\|} = |\lambda(\tilde{M}^k[t])| \leq \rho(\tilde{M}^k[t]), \tag{45}$$

which results in  $\|x^k[t+1]\| \leq [1 - h \min_{i \in [n]} \{\gamma_i^k\}] \|x^k[t]\|$  for all  $t$ . Since,  $\gamma_i^k > 0$  for all  $i \in [n], k \in [m]$ , from Assumption 2, we obtain that, for all  $x_i^k[0] \in [0, 1]^n$ ,

$$\|x^k[t]\| \leq [1 - h \min_{i \in [n]} \{\gamma_i^k\}]^t \|x^k[0]\| \leq e^{-th \min_{i \in [n]} \{\gamma_i^k\}} \|x^k[0]\|, \quad (46)$$

where the second inequality holds by Bernoulli's inequality [62]. Hence,  $x^k[t]$  converges to  $\mathbf{0}$  with at least an exponential rate of  $h \min_{i \in [n]} \{\gamma_i^k\}$ , according to Proposition 1.  $\square$

**Corollary 4.** *If we apply the mitigation strategy in Theorem 4 to all viruses  $k \in [m]$ , then the system in (2) converges to the healthy state at an exponential rate.*

**Remark 5.** *The control strategy proposed in Theorem 4 can be interpreted as follows: if the healing rate with respect to virus  $k$  of each subpopulation is appropriately increased according to the susceptible level, for example by distributing effective medication, medical supplies, and healthcare workers to each subpopulation, then the epidemic will be eradicated at an exponential rate. This theorem provides decision-makers insight into, given sufficient resources, how to allocate medical supplies and healthcare workers to different subpopulations so that the epidemic can be eradicated quickly. Moreover, notice that the convergence rate of virus  $k$  depends on the minimum healing rate at each node of the network corresponding to the  $k$ -th virus, which encourages the decision-makers to elevate the lowest healthcare level of the subpopulation within the community.*

Our feedback controller (42) is an improvement with respect to similar *open-loop* control schemes for networked SIS models in [17], [61], [65], since it does not require full information of the system states. More specifically, for the feedback gain design, because the recovered state can be calculated using  $r_i[t] = h \sum_{q=0}^t \sum_{k=1}^m \gamma_i^k x_i^k[q]$ , we only need knowledge of the susceptible level  $s_i[t]$  or knowledge of the infected level,  $x_i^k[t]$  for all  $k \in [m], i \in [n]$ . Furthermore, compared to the control strategies proposed in [17], [61], [65] whose boosted healing rates maintain constant values, our distributed feedback controller, since it updates the healing rates in response to the infection level in a subpopulation, is capable of allocating the medical resource more efficiently. In the next section, among other results, we will explore the performance of our distributed feedback controller by relying only on the estimates of the system states in addition to the actual system states.

## VI. SIMULATIONS

In this section, we consider the special case of two competing variants of the SARS-CoV-2 virus, (i.e.  $m = 2$ ): Delta and Omicron spreading over the network depicted in Figure 2 [66]. We choose the two variants of the SARS-CoV-2 virus because they cause patients to display similar symptoms such as fever, coughing, and headache [41], [42]. We consider a network of 5 nodes, where each node represents a country in Europe: France, Italy, Switzerland, Austria, and Germany; there exists an edge between two nodes if the countries that the nodes represent share a border with each other. The system



FIGURE 2: Contact graph for the spread of the Omicron and Delta variants of SARS-CoV-2 virus.

parameters corresponding to the two variants of SARS-CoV-2 virus are listed in Table I and Table II, respectively. This section includes no real data; however, the viral spreading parameters are inspired by the behavior of the viruses [67], that is, the model parameters are chosen so that the Omicron variant is more contagious than Delta. We also acknowledge that these two variants are not necessarily competitive; there are cases where people have been infected with both variants. However, the samples of co-infection of both variants are very uncommon [68], thus can be disregarded in the population and the time scales being considered in these simulations.

$\beta_{ij}^1$	FR	IT	CH	AT	DE
FR	0.08	0.15	0.24	0	0.06
IT	0.15	0.12	0.13	0.11	0
CH	0.24	0.13	0.25	0.05	0.04
AT	0	0.09	0.05	0.11	0.15
DE	0.06	0	0.04	0.14	0.09
$\gamma_i^1$	0.15	0.23	0.17	0.25	0.2
$x^1[0]$	0.005	0.01	0.0075	0.0025	0.0075
$c^1$	0.4	0.4	0.4	0.4	0.4

TABLE I: For the network in Figure 2, disease parameters corresponding to the Omicron variant.

$\beta_{ij}^2$	FR	IT	CH	AT	DE
FR	0.02	0.05	0.04	0	0.01
IT	0.05	0.06	0.07	0.02	0
CH	0.04	0.07	0.04	0.03	0.05
AT	0	0.03	0.04	0.09	0.07
DE	0.01	0	0.05	0.07	0.06
$\gamma_i^2$	0.095	0.12	0.1	0.15	0.13
$x^2[0]$	0.001	0.002	0.0035	0.002	0.001
$c^2$	0.3	0.3	0.3	0.3	0.3

TABLE II: For the network in Figure 2, disease parameters corresponding to the Delta variant.

The evolution of the infection levels of both viruses are illustrated in Figure 3, and the effective reproduction number, namely  $\rho(\tilde{M}^k[t])$ , of both viruses are plotted in Figure 4. The infection level of each virus attains its peak at the same time when  $\rho(\tilde{M}^k[t])$  drops down to 1, consistent with our analysis

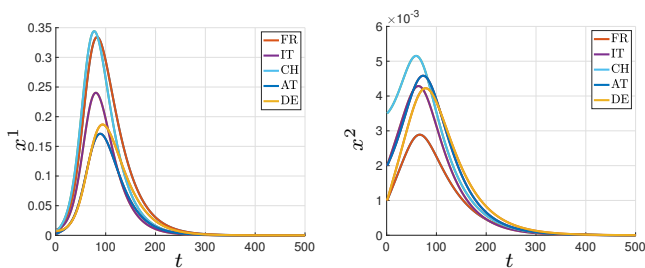


FIGURE 3: Evolution of infection level of the Omicron variant in each country (left); Evolution of infection level of the Delta variant in each country (right).

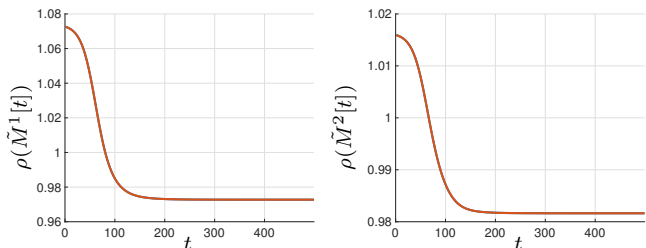


FIGURE 4: Spectral Radius of the state transition matrix of the Omicron variant in each country (left); Spectral Radius of the state transition matrix of the Delta variant in each country (right).

in Section III. We plot the total fraction of individuals who exhibit similar symptoms that are caused due to either of the viruses, namely  $y_i[t]$ , with  $i \in [5]$ , from the observation model in Eq. (4); see Figure 5.

We then estimate the infection level by using the Luenberger observer of Eq. (28), with  $\hat{s}[t]$  and  $\hat{r}[t]$  calculated via Eq. (26) and Eq. (27), respectively. The initial conditions are provided in Table III. To investigate the impact of the observer gain  $L_i^k$  on the estimation error, we simulate the Luenberger observer's performance with a scaled observer gain  $\eta L_i^k$ , where  $L_i^k = 1$ ,

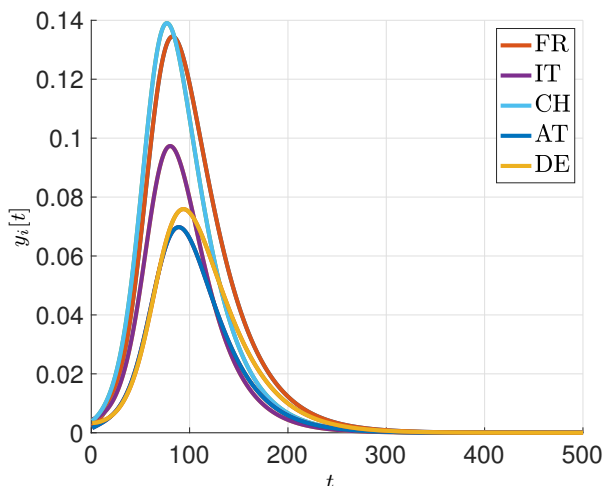


FIGURE 5: Total proportion of individuals who show similar symptoms from both variants in each country.

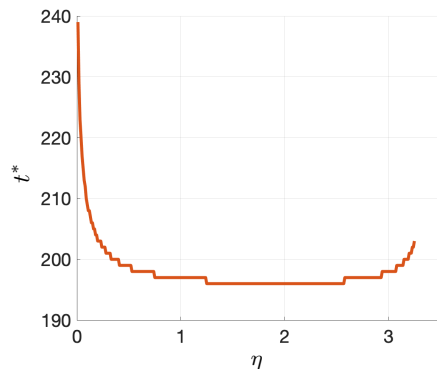


FIGURE 6: The scale of the observer gain vs the time for the estimation error to converge to zero.

for all  $i \in [5], k \in [2]$ . Let  $t^*$  denote the time instant such that the aggregated estimation error  $\frac{1}{mn} \sum_{k=1}^m \sum_{i=1}^n |x_i^k[t] - \hat{x}_i^k[t]| < 0.01$ , for all  $t > t^*$ . In Figure 6, we illustrate how the point in time at which the estimation error converges ( $t^*$ ) depends on the gain of the observer ( $\eta$ ) for this system. We can see that as the observer gain increases, the convergence time first decreases and then increases; eventually,  $t^*$  no longer exists because a large observer gain can cause the estimated infection level to exceed 1, that is, the estimated system states cease to be well-defined. In Figure 6, when the scale of the observer gain  $\eta > 3.3$ , the estimated infection level  $\hat{x}_i^k[t] \rightarrow \infty$  as  $t$  increases.

We next focus on finding the feasible observer gain  $L^k$  such that the systems states are well-defined. We set  $\tau^1 = 0.1$  and  $\tau^2 = 0.3$ , where  $\tau^k$ , for each  $k \in [2]$ , is as defined in Theorem 3. For different  $l^k$  values, we calculate the corresponding  $L^k$  values using LMI (41). It turns out that setting  $l^k = 10^{10}$  for both viruses ensures that all the estimated system states are well-defined. Note that the feasible value of  $l^k$  is not unique. For our subsequent simulations, we set  $l^k = 10^{10}$ , and, by solving the LMI (41) in Corollary 3, we obtain the observer gain  $L^k$ :

$$L^1 = \begin{bmatrix} 0.101223398722677 \\ 0.0928658303375023 \\ 0.112524328507691 \\ 0.0860241631907317 \\ 0.0843783515296357 \end{bmatrix}, L^2 = \begin{bmatrix} 0.0853417070451051 \\ 0.0879525432030855 \\ 0.0898592088737154 \\ 0.0885900881539504 \\ 0.0897704274804431 \end{bmatrix}. \quad (47)$$

Notice that  $\|L^2\| < \|L^1\|$ . Thus, we need less compensation from the observer gain for the system state estimation of Delta than for that of Omicron.

We now explore whether we are able to retrieve the observer gains for all viruses through LMI (41), when the assumptions in Theorem 2 are not satisfied. If we set  $\gamma_{DE}^2 = \gamma_{DE}^1 = 0.2$  in Table II, then the LMI (41) becomes infeasible for the Delta variant, hence we are not able to accurately estimate the infection level for the Delta variant. Therefore, when the healing rates of different viruses are identical at a node, we are unable to find the appropriate observer gain, which can be interpreted as saying that we are not able to estimate the system states of each virus if the viruses are indistinguishable (i.e., the recovery rates for the two viruses are the same) from

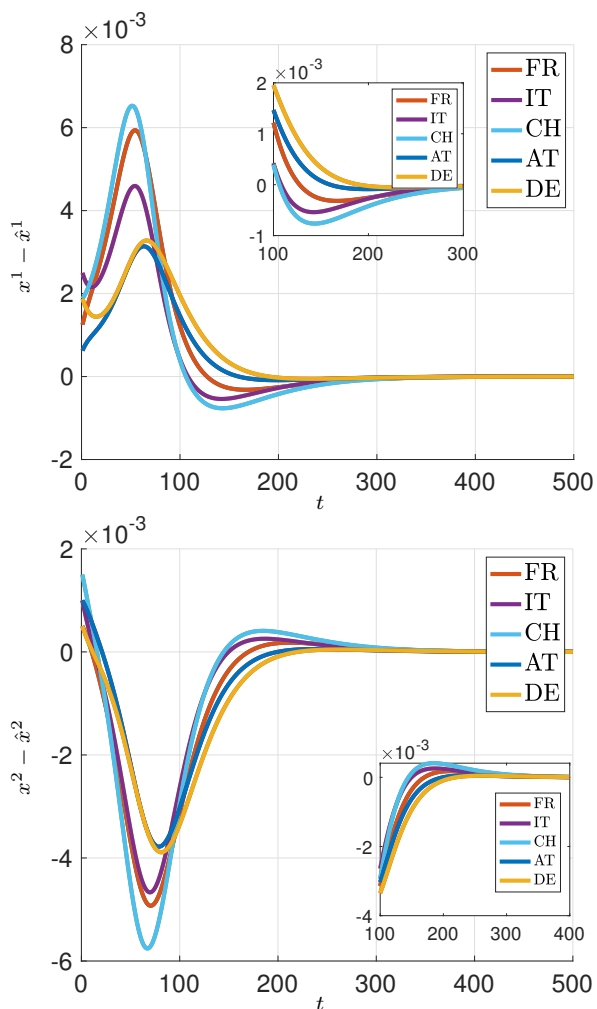


FIGURE 7: Estimation error of infection level of the Omicron variant in each country (top); Estimation error of infection level of the Delta variant in each country (bottom).

each other at any subpopulation, consistent with Theorem 2.

	FR	IT	CH	AT	DE
$\hat{x}^1[0]$	0.0037	0.0075	0.0056	0.0019	0.0056
$\hat{x}^2[0]$	0.0005	0.001	0.002	0.001	0.0005

TABLE III: Initial conditions assumed for the Luenberger observer (28).

To evaluate the performance of our proposed estimation algorithm, we simulate the state estimation errors, with observer gains from (47) and initial conditions from Table III, in Figure 7. We can see that, in Figure 7 (top), the estimation error of the Omicron variant is negligible compared to its infection level, and converges to zero before its infection level does. In Figure 7 (bottom), the estimation error of the Delta variant starts to die out around  $t = 250$ ; while the infection levels converge to zero when  $t > 300$ , as seen in Figure 3 (right). Hence, the simulation results in Figure 7 are consistent with Theorem 3.

Inspired by Corollary 2, we now explore how to properly choose the Lipschitz-like constant  $l^k$  for our model by denot-

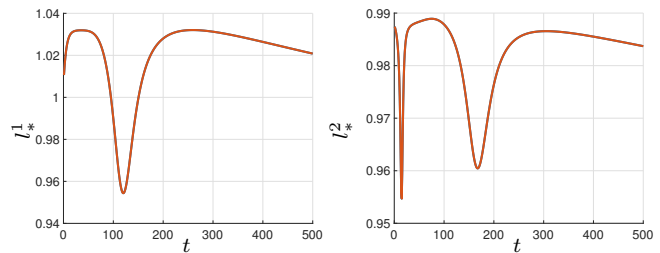


FIGURE 8: Lipschitz-like constant  $l_*^k$  of the Omicron variant in each country (left); Lipschitz-like constant  $l_*^k$  of the Delta variant in each country (right).

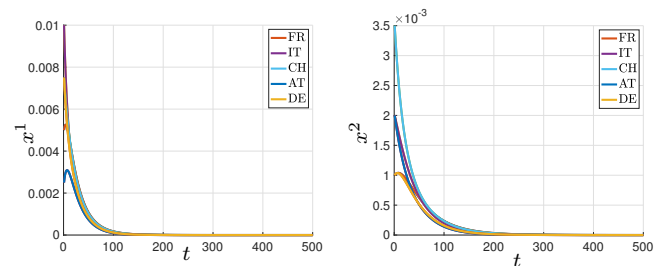


FIGURE 9: Evolution of infection level of the Omicron variant in each country with the distributed feedback control strategy in Eq. (42) (left); Evolution of infection level of the Delta variant in each country the distributed feedback control strategy in Eq. (42) (right).

ing:

$$l_*^k[t] = \frac{\|w^k[t]\|}{\|x^k[t] - \hat{x}^k[t]\|} \quad (48)$$

for all  $k \in [2]$ . In Figure 8, we plot the Lipschitz-like constant  $l_*^k[t]$  of our network (see Figure 2) for both viruses over time. Recall from Corollary 2 that we must choose  $l^k$  such that, for each  $k \in [2]$ :

$$l^k \geq \frac{\|w^k[t]\|}{\|x^k[t] - \hat{x}^k[t]\|} \quad (49)$$

for all  $t \in \mathbb{Z}_{\geq 0}$ . Our choice of  $l^k = 10^{10} > l_*^k[t]$  for all  $t \in \mathbb{Z}_{\geq 0}$ , as seen in Figure 8, satisfies the requirement of Corollary 2.

In Figure 9, we implement the distributed feedback mitigation strategy of Eq. (42) over all the countries in our network. We can see that, consistent with Theorem 4, our proposed mitigation strategy is able to eradicate the spread of both viruses at an exponential rate. Moreover, maintaining the mitigation strategy over the network throughout time ensures that no subsequent infection wave occurs. We then explore the state feedback controller of Eq. (42) which utilizes the estimated system states instead of the actual system states, i.e., the control input is calculated as:

$$\bar{u}_i^k[t] = -\hat{s}_i[t] \sum_{j=1}^n \beta_{ij}^k, \quad (50)$$

where  $\hat{s}_i[t]$  is obtained through the estimation algorithm in Eq. (28). In Figure 10, we plot the infection level for both viruses using the mitigation strategy (42) with the control

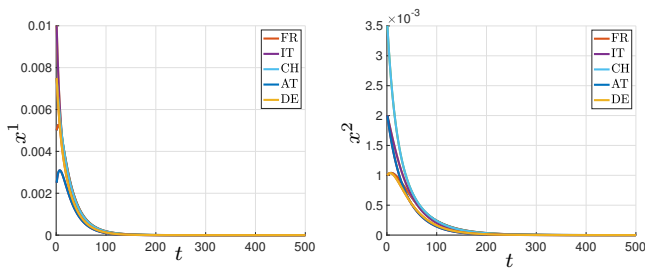


FIGURE 10: Evolution of the infection level of the Omicron variant in each country with the distributed mitigation strategy with a control input from Eq. (50) (left); Evolution of the infection level of the Delta variant in each country with the distributed mitigation strategy with a control input from Eq. (50) (right).

input (50) applied. It can be seen that the feedback controller with the estimated states is able to achieve the same goal, namely, eradicating each virus at an exponential rate. Even though Theorem 4 did not prove that the feedback controller that uses the estimated susceptible level Eq. (50) eradicates the viruses at an exponential rate, it seems that our estimation algorithm in Eq. (28) is able to reconstruct the susceptible level accurately in order to enable rapid eradication in this case.

## VII. CONCLUSION

This paper has proposed a novel discrete-time networked multi-virus SIR model. We have provided two sufficient conditions for each virus to converge to zero exponentially. Then, we have specified a sufficient condition for the system to be strongly locally observable when there are no susceptible individuals in the network. We have proposed a distributed Luenberger observer which estimates the system states. We have then provided a method for choosing the observer gain such that the estimation error of each virus converges to zero asymptotically. We have introduced a distributed feedback mitigation strategy that ensured that each virus is eradicated at an exponential rate. In the simulations, we have utilized the Luenberger state observer proposed to estimate the system states and the results illustrate that the Luenberger observer is suitable for state estimation of our model.

For future work, we plan to study the observability of the system by relaxing the assumption that all nodes have zero susceptible individuals and allowing for more realistic and generic susceptible levels. In addition, we would like to explore the system state estimation problem in the presence of measurement noise to emulate practical scenarios where there is error in the collected data. We also aim to study more complex models, such as the SEIR and SAIR models, which incorporate additional compartments for exposed or asymptomatic individuals.

## REFERENCES

[1] C. Zhang, S. Gracy, T. Başar, and P. E. Paré, “A networked competitive multi-virus SIR model: Analysis and observability,” *IFAC-PapersOnLine*, vol. 55, no. 13, pp. 13–18, 2022.

[2] O. J. Benedictow and O. L. Benedictow, *The Black Death, 1346-1353: The Complete History*. Boydell & Brewer, 2004.

[3] K. Cheng and P. Leung, “What happened in China during the 1918 influenza pandemic?” *International Journal of Infectious Diseases*, vol. 11, no. 4, pp. 360–364, 2007.

[4] N. P. Johnson and J. Mueller, “Updating the accounts: Global mortality of the 1918-1920 Spanish influenza pandemic,” *Bulletin of the History of Medicine*, pp. 105–115, 2002.

[5] World Health Organization (WHO), “2009 H1N1 Pandemic,” <https://www.cdc.gov/flu/pandemic-resources/2009-h1n1-pandemic.html>, accessed: 2022-12-08.

[6] —, “Global coronavirus (2019-nCoV),” <https://www.who.int/emergencies/diseases/novel-coronavirus-2019>, accessed: 2022-12-08.

[7] W. Mei, S. Mohagheghi, S. Zampieri, and F. Bullo, “On the dynamics of deterministic epidemic propagation over networks,” *Annual Reviews in Control*, vol. 44, pp. 116–128, 2017.

[8] H. H. Weiss, “The SIR model and the foundations of public health,” *Materials Mathematics*, pp. 0001–17, 2013.

[9] V. Colizza, A. Barrat, M. Barthélemy, and A. Vespignani, “Predictability and epidemic pathways in global outbreaks of infectious diseases: the sars case study,” *BMC Medicine*, vol. 5, no. 1, pp. 1–13, 2007.

[10] H.-J. Chang, “Estimation of basic reproduction number of the Middle East respiratory syndrome coronavirus (MERS-CoV) during the outbreak in South Korea, 2015,” *Biomedical Engineering Online*, vol. 16, no. 1, pp. 1–11, 2017.

[11] D. Osthus, K. S. Hickmann, P. C. Caragea, D. Higdon, and S. Y. Del Valle, “Forecasting seasonal influenza with a state-space SIR model,” *The Annals of Applied Statistics*, vol. 11, no. 1, p. 202, 2017.

[12] B. J. Coburn, B. G. Wagner, and S. Blower, “Modeling influenza epidemics and pandemics: Insights into the future of swine flu (H1N1),” *BMC Medicine*, vol. 7, no. 1, pp. 1–8, 2009.

[13] T. Berge, J.-S. Lubuma, G. Moremedi, N. Morris, and R. Kondera-Shava, “A simple mathematical model for Ebola in Africa,” *Journal of Biological Dynamics*, vol. 11, no. 1, pp. 42–74, 2017.

[14] G. C. Calafiore, C. Novara, and C. Possieri, “A modified SIR model for the COVID-19 contagion in Italy,” in *Proc. 59th IEEE Conference on Decision and Control (CDC)*. IEEE, 2020, pp. 3889–3894.

[15] Y.-C. Chen, P.-E. Lu, C.-S. Chang, and T.-H. Liu, “A time-dependent SIR model for COVID-19 with undetectable infected persons,” *IEEE Transactions on Network Science and Engineering*, vol. 7, no. 4, pp. 3279–3294, 2020.

[16] S. Gracy, P. E. Paré, J. Liu, H. Sandberg, C. L. Beck, K. H. Johansson, and T. Başar, “Modeling and analysis of a coupled SIS bi-virus model,” *Automatica*, <https://arxiv.org/pdf/2207.11414.pdf>, 2022, Note: Under Review, 2<sup>nd</sup> Round.

[17] J. Liu, P. E. Paré, A. Nedić, C. Y. Tang, C. L. Beck, and T. Başar, “Analysis and control of a continuous-time bi-virus model,” *IEEE Transactions on Automatic Control*, vol. 64, no. 12, pp. 4891–4906, 2019.

[18] M. Ye, B. D. Anderson, and J. Liu, “Convergence and equilibria analysis of a networked bivirus epidemic model,” *SIAM Journal on Control and Optimization*, vol. 60, no. 2, pp. S323–S346, 2022.

[19] K. M. Pepin, K. Lambeth, and K. A. Hanley, “Asymmetric competitive suppression between strains of dengue virus,” *BMC Microbiology*, vol. 8, no. 1, pp. 1–10, 2008.

[20] M. Nowak, “The evolution of viruses. competition between horizontal and vertical transmission of mobile genes,” *Journal of Theoretical Biology*, vol. 150, no. 3, pp. 339–347, 1991.

[21] A. M. Poland, H. Vennema, J. E. Foley, and N. C. Pedersen, “Two related strains of feline infectious peritonitis virus isolated from immunocompromised cats infected with a feline enteric coronavirus,” *Journal of Clinical Microbiology*, vol. 34, no. 12, pp. 3180–3184, 1996.

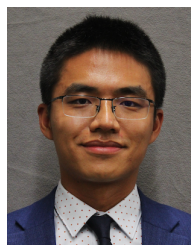
[22] P. Van Mieghem, J. Omic, and R. Kooij, “Virus spread in networks,” *IEEE/ACM Trans. on Net.*, vol. 17, no. 1, pp. 1–14, 2009.

[23] P. E. Paré, J. Liu, C. L. Beck, A. Nedić, and T. Başar, “Multi-competitive viruses over static and time-varying networks,” in *Proceedings of the 2017 American Control Conference (ACC)*. IEEE, 2017, pp. 1685–1690.

[24] B. A. Prakash, A. Beutel, R. Rosenfeld, and C. Faloutsos, “Winner takes all: Competing viruses or ideas on fair-play networks,” in *Proceedings of the 21st International Conference on World Wide Web*, 2012, pp. 1037–1046.

[25] P. E. Paré, D. Vrabac, H. Sandberg, and K. H. Johansson, “Analysis, online estimation, and validation of a competing virus model,” in *Proceedings of the 2020 American Control Conference (ACC)*. IEEE, 2020, pp. 2556–2561.

- [26] F. D. Sahneh and C. Scoglio, "Competitive epidemic spreading over arbitrary multilayer networks," *Physical Review E*, vol. 89, no. 6, p. 062817, 2014.
- [27] A. Santos, J. M. Moura, and J. M. Xavier, "Bi-virus SIS epidemics over networks: Qualitative analysis," *IEEE Transactions on Network Science and Engineering*, vol. 2, no. 1, pp. 17–29, 2015.
- [28] J. Liu, P. E. Paré, A. Nedić, C. Y. Tang, C. L. Beck, and T. Başar, "On the analysis of a continuous-time bi-virus model," in *Proceedings of the 2016 IEEE 55th Conference on Decision and Control (CDC)*. IEEE, 2016, pp. 290–295.
- [29] P. E. Paré, J. Liu, C. L. Beck, A. Nedić, and T. Başar, "Multi-competitive viruses over time-varying networks with mutations and human awareness," *Automatica*, vol. 123, p. 109330, 2021.
- [30] A. Janson, S. Gracy, P. E. Paré, H. Sandberg, and K. H. Johansson, "Networked multi-virus spread with a shared resource: Analysis and mitigation strategies," *arXiv preprint arXiv:2011.07569*, 2020.
- [31] C. Zhang, H. Leung, B. Butler, and P. Paré, "Estimation and distributed eradication of SIR epidemics on networks," *arXiv preprint arXiv:2102.12549*, 2021.
- [32] H. Ito, "Strict smooth Lyapunov Functions and vaccination control of the SIR model certified by ISS," *IEEE Transactions on Automatic Control*, vol. 67, no. 9, pp. 4514–4528, 2022.
- [33] B. She, H. C. Leung, S. Sundaram, and P. E. Paré, "Peak infection time for a networked SIR epidemic with opinion dynamics," in *Proceedings of the 60th IEEE Conference on Decision and Control (CDC)*. IEEE, 2021, pp. 2104–2109.
- [34] B. She, S. Sundaram, and P. E. Paré, "A learning-based model predictive control framework for real-time SIR epidemic mitigation," in *Proceedings of the 2022 American Control Conference (ACC)*. IEEE, 2022, pp. 2565–2570.
- [35] K. D. Smith and F. Bullo, "Convex optimization of the basic reproduction number," *IEEE Transactions on Automatic Control*, 2022.
- [36] A. Ignatov and S. Trigger, "Two viruses competition in the SIR model of epidemic spread: Application to COVID-19," *MedRxiv preprint doi: <https://doi.org/10.1101/2022.01.11.2022>*, vol. 11, 2022.
- [37] J. Lopez Bernal, N. Andrews, C. Gower, E. Gallagher, R. Simmons, S. Thelwall, J. Stowe, E. Tessier, N. Groves, G. Dabrera *et al.*, "Effectiveness of COVID-19 vaccines against the B. 1.617. 2 (Delta) variant," *New England Journal of Medicine*, 2021.
- [38] G. D. Barmparis and G. Tsironis, "Estimating the infection horizon of COVID-19 in eight countries with a data-driven approach," *Chaos, Solitons & Fractals*, vol. 135, p. 109842, 2020.
- [39] T. W. Russell, J. Hellewell, C. I. Jarvis, K. Van Zandvoort, S. Abbott, R. Ratnayake, S. Flasche, R. M. Eggo, W. J. Edmunds, A. J. Kucharski *et al.*, "Estimating the infection and case fatality ratio for coronavirus disease (COVID-19) using age-adjusted data from the outbreak on the Diamond Princess cruise ship, February 2020," *Eurosurveillance*, vol. 25, no. 12, p. 2000256, 2020.
- [40] G. Meyerowitz-Katz and L. Merone, "A systematic review and meta-analysis of published research data on COVID-19 infection-fatality rates," *International Journal of Infectious Diseases*, 2020.
- [41] M. Antonelli, J. C. Pujol, T. D. Spector, S. Ourselin, and C. J. Steves, "Risk of long COVID associated with Delta versus Omicron variants of SARS-CoV-2," *The Lancet*, vol. 399, no. 10343, pp. 2263–2264, 2022.
- [42] B. Rader, A. Gertz, A. D. Iuliano, M. Gilmer, L. Wronski, C. M. Astley, K. Sewalk, T. J. Varrelman, J. Cohen, R. Parikh *et al.*, "Use of at-home COVID-19 tests—United States, August 23, 2021–March 12, 2022," *Morbidity and Mortality Weekly Report*, vol. 71, no. 13, p. 489, 2022.
- [43] R. Perks and N. Schneek, "COVID-19 in artisanal and small-scale mining communities: Preliminary results from a global rapid data collection exercise," *Environmental Science & Policy*, vol. 121, pp. 37–41, 2021.
- [44] S. Ma, F. Zhang, F. Zhou, H. Li, W. Ge, R. Gan, H. Nie, B. Li, Y. Wang, M. Wu *et al.*, "Metagenomic analysis reveals oropharyngeal microbiota alterations in patients with COVID-19," *Signal Transduction and Targeted Therapy*, vol. 6, no. 1, pp. 1–11, 2021.
- [45] E. A. Belongia and M. T. Osterholm, "COVID-19 and flu, a perfect storm," pp. 1163–1163, 2020.
- [46] M. U. B. Niazi and K. H. Johansson, "Observer design for the state estimation of epidemic processes," in *Proceedings of the 61st IEEE Conference on Decision and Control (CDC)*, 2022.
- [47] G. I. Bara, A. Zemouche, and M. Boutayeb, "Observer synthesis for Lipschitz discrete-time systems," in *Proceedings of the 2005 IEEE International Symposium on Circuits and Systems*. IEEE, 2005, pp. 3195–3198.
- [48] M. Arcak and P. Kokotović, "Nonlinear observers: A circle criterion design and robustness analysis," *Automatica*, vol. 37, no. 12, pp. 1923–1930, 2001.
- [49] A. Mitra and S. Sundaram, "Distributed observers for LTI systems," *IEEE Transactions on Automatic Control*, vol. 63, no. 11, pp. 3689–3704, 2018.
- [50] J. Snow, *On the Mode of Communication of Cholera*. John Churchill, 1855.
- [51] WHO, "Ebola virus disease – Democratic Republic of the Congo," <https://www.who.int/csr/don/30-january-2020-ebola-drc/en/>, accessed: 2020-02-03.
- [52] K. E. Atkinson, *An Introduction to Numerical Analysis*. John Wiley & sons, 2008.
- [53] F. Brauer, C. Castillo-Chavez, and Z. Feng, *Mathematical Models in Epidemiology*. Springer, 2019, vol. 32.
- [54] P. F. Teunis, C. L. Moe, P. Liu, S. E. Miller, L. Lindesmith, R. S. Baric, J. Le Pendu, and R. L. Calderon, "Norwalk virus: how infectious is it?" *Journal of Medical Virology*, vol. 80, no. 8, pp. 1468–1476, 2008.
- [55] J. Panovska-Griffiths, C. C. Kerr, R. M. Stuart, D. Mistry, D. J. Klein, R. M. Viner, and C. Bonell, "Determining the optimal strategy for reopening schools, the impact of test and trace interventions, and the risk of occurrence of a second COVID-19 epidemic wave in the UK: A modelling study," *The Lancet Child & Adolescent Health*, vol. 4, no. 11, pp. 817–827, 2020.
- [56] M. Vidyasagar, *Nonlinear Systems Analysis*. SIAM, 2002.
- [57] W. J. Rugh, *Linear System Theory*. Prentice Hall Upper Saddle River, NJ, 1996, vol. 2.
- [58] A. Rantzer, "Distributed control of positive systems," in *Proceedings of the 50th IEEE Conference on Decision and Control and European Control Conference*, 2011, pp. 6608–6611.
- [59] E. D. Sontag, "On the observability of polynomial systems, I: Finite-time problems," *SIAM Journal on Control and Optimization*, vol. 17, no. 1, pp. 139–151, 1979.
- [60] H. Nijmeijer, "Observability of autonomous discrete time non-linear systems: a geometric approach," *International Journal of Control*, vol. 36, no. 5, pp. 867–874, 1982.
- [61] S. Gracy, P. E. Paré, H. Sandberg, and K. H. Johansson, "Analysis and distributed control of periodic epidemic processes," *IEEE Transactions on Control of Network Systems*, vol. 8, no. 1, pp. 123–134, 2020.
- [62] N. L. Carothers, *Real Analysis*. Cambridge University Press, 2000.
- [63] R. J. Whitley and B. Roizman, "Herpes simplex virus infections," *The Lancet*, vol. 357, no. 9267, pp. 1513–1518, 2001.
- [64] F. Zhang, *The Schur Complement and its Applications*. Springer Science & Business Media, 2006, vol. 4.
- [65] M. Ye, J. Liu, B. D. Anderson, and M. Cao, "Applications of the Poincaré–Hopf Theorem: Epidemic Models and Lotka–Volterra Systems," *IEEE Transactions on Automatic Control*, vol. 67, no. 4, pp. 1609–1624, 2021.
- [66] C. M. Zipfel, V. Colizza, and S. Bansal, "The missing season: The impacts of the COVID-19 pandemic on influenza," *Vaccine*, vol. 39, no. 28, pp. 3645–3648, 2021.
- [67] L. B. Shrestha, C. Foster, W. Rawlinson, N. Tedla, and R. A. Bull, "Evolution of the SARS-CoV-2 Omicron variants BA. 1 to BA. 5: Implications for immune escape and transmission," *Reviews in Medical Virology*, vol. 32, no. 5, p. e2381, 2022.
- [68] A. Bolze, T. Basler, S. White, A. Dei Rossi, D. Wyman, H. Dai, P. Roychoudhury, A. L. Greninger, K. Hayashibara, M. Beatty *et al.*, "Evidence for SARS-CoV-2 Delta and Omicron co-infections and recombination," *Med*, vol. 3, no. 12, pp. 848–859, 2022.



**Ciyuan Zhang** is a Ph.D. student in the School of Electrical and Computer Engineering at Purdue University. He received his M.S. in Electrical Engineering from Columbia University in 2018 and his B.S. in Electrical Engineering from Xi'an Jiaotong University in 2016. He is a recipient of Purdue University's Bilsland Dissertation Fellowship. His research interests include estimating and controlling epidemic dynamics on networked systems.



**Sebin Gracy** is a Post-Doctoral Associate in the Department of Electrical and Computer Engineering at Rice University, Houston, TX. Previously, he was a Post-Doctoral Researcher in the Division of Decision and Control Systems in the School of Electrical Engineering and Computer Science at KTH Royal Institute of Technology. He obtained his Ph.D. degree at Université Grenoble-Alpes in November, 2018. Prior to that, he obtained his M.S. and B.E. degrees in Electrical Engineering from the University of Colorado at Boulder and the University of Mumbai, in December, 2013 and June 2010, respectively. His research focuses on networked dynamical systems, with a particular emphasis on the theory of spreading processes.



**Tamer Başar** (S'71-M'73-SM'79-F'83-LF'13) is with the University of Illinois at Urbana-Champaign (UIUC), where he holds the academic positions of Swanlund Endowed Chair Emeritus; Center for Advanced Study Professor Emeritus of Electrical and Computer Engineering; Research Professor at the Coordinated Science Laboratory; and Research Professor at the Information Trust Institute. He received B.S.E.E. from Robert College, Istanbul, and M.S., M.Phil, and Ph.D. from Yale University. He is a member of the US National Academy of Engineering, a member of the American Academy of Arts and Sciences, and Fellow of IEEE, IFAC and SIAM, and has served as president of IEEE CSS, ISDG, and AACC. He has received several awards and recognitions over the years, including the highest awards of IEEE CSS, IFAC, AACC, and ISDG; the IEEE Control Systems Award; and a number of international honorary doctorates and professorships. He has over 1000 publications in systems, control, communications, and dynamic games, including books on non-cooperative dynamic game theory, robust control, network security, wireless and communication networks, and stochastic networked control. He was the Editor-in-Chief of *Automatica* between 2004 and 2014, and is currently editor of several book series. His current research interests include stochastic teams, games, and networks; multi-agent systems and learning; spread of misinformation and epidemics; security; and cyber-physical systems.



**Philip E. Paré** (Member, IEEE) is an Assistant Professor in the School of Electrical and Computer Engineering at Purdue University. He received his Ph.D. in Electrical and Computer Engineering (ECE) from the University of Illinois at Urbana-Champaign (UIUC) in 2018, after which he went to KTH Royal Institute of Technology in Stockholm, Sweden to be a Post-Doctoral Scholar. He received his B.S. in Mathematics with University Honors and his M.S. in Computer Science from Brigham Young University in 2012 and 2014, respectively. He is a recipient of the NSF CAREER award and was an inaugural Societal Impact Fellow at Purdue. His research focuses on networked control systems, namely modeling, analysis, and control of virus spread over networks.